Quaternary International 434 (2017) 84–91

Contents lists available at ScienceDirect

Quaternary International

journal homepage: www.elsevier.com/locate/quaint

The age of human remains and associated fauna from Zhiren Cave in Guangxi, southern China

Yanjun Cai [a, *], Xiaoke Qiang [a], Xulong Wang [a], Changzhu Jin [b], Yuan Wang [b], Yingqi Zhang [b], Erik Trinkaus [c], Zhisheng An [a]

[a] State Key Laboratory of Loess and Quaternary Geology, Institute of Earth Environment, Chinese Academy of Sciences, Xi'an 710075, China
[b] Key Laboratory of Vertebrate Evolution and Human Origins of Chinese Academy of Sciences, Institute of Vertebrate Paleontology and Paleoanthropology, Chinese Academy of Sciences, Beijing 100044, China
[c] Department of Anthropology, Washington University, St. Louis, MO 63130, USA

ARTICLE INFO

Article history:
Available online 24 March 2016

Keywords:
Zhiren Cave
Human remains
Paleomagnetic stratigraphy
Asian elephant fauna
Chronology

ABSTRACT

Zhiren Cave in southern China is an important site for the study of the origin and the environmental background of early modern humans. The combination of *Elephas kiangnanensis*, *Elephas maximus*, and *Megatapirus augustus*, indicates an early representative of the typical Asian elephant fauna. Previous U-series dating of flowstone calcite has pinpointed an upper age limit for the fossils of about 100 ka. In order to achieve a better comprehension of the chronology of the modern human and contemporaneous faunal assemblage, paleomagnetic, stratigraphic, and optically stimulated luminescence (OSL) dating methods have been applied to the cave sediments. Paleomagnetic analyses reveal that there is a reversed polarity excursion below the fossiliferous layer. This excursion can be regarded as the Blake excursion event, given the U-series ages of the overlying flowstone calcite, the OSL measurements, the virtual geomagnetic pole (VGP) path of the excursion, the two reverse polarity zones within this excursion event, and the characteristic of the fauna assemblage. The human remains and mammalian fauna assemblage can be bracketed to 116–106 ka. Application of OSL dating leads to erroneous ages, largely due to the uncertainty associated with the estimation on the dose rates.

1. Introduction

The later part of the Middle Pleistocene and the early Late Pleistocene saw the transition in eastern Asia from an archaic fauna with a large percentage of currently extinct mammals to faunal assemblages dominated by extant species (Jin et al., 2009; Zhao et al., 2009; Wang et al., 2010). This is increasingly evident in a series of cave sites in southern China, in which there is a shift from the typical Middle Pleistocene *Ailuropoda-Stegodon* (*sensu stricto*) assemblages to a fauna dominated by *Elephas maximus* and other extant species (Jin et al., 2009).

Among the paleontological transitions is the emergence of early modern humans (*Homo sapiens sensu stricto*) in the region, a morphotype distinct from late archaic humans that is first apparent in the late Middle Pleistocene (MIS 6) of equatorial Africa and then subsequently appears during the Late Pleistocene (MIS 5 to 3) across Eurasia (Trinkaus, 2005). The current consensus is that the Late Pleistocene emergence of early modern humans across Eurasia involved dispersal of those African early modern humans combined with regionally and temporally variable degrees of assimilation of regional late archaic humans, based on both morphological (Smith et al., 2005; Trinkaus, 2007; Shang and Trinkaus, 2010) and molecular (Fu et al., 2013, 2014, 2015) paleontological data. In some regions, the degree of late archaic human assimilation may have approached the equivalent of regional continuity across the late archaic to early modern human transition, albeit with substantial gene flow from elsewhere (Wu, 2004).

The details of both of these transitions in east Asia, one general mammalian and the other in the genus *Homo*, are still unclear, in large part due to the dearth of later Middle and earlier Late Pleistocene fossil assemblages that are securely bracketed in time. This ongoing issue is being slowly remedied by improvements in

* Corresponding author.
E-mail address: yanjun_cai@ieecas.cn (Y. Cai).

http://dx.doi.org/10.1016/j.quaint.2015.12.088
1040-6182/

the application of dating techniques and the discovery of new and datable fossil assemblages. Among the latter is the paleontologically rich Zhiren Cave (Zhirendong, *Homo sapiens* Cave), located in the Mulanshan (Mulan Mountain), Chongzuo City, Guangxi Zhuang Autonomous Region in southern China (22°17′13.6″N; 107°30′45.1″E, Jin et al., 2009). A rich large and small mammalian assemblage has been unearthed, as well as three elements (two molars and a partial mandible) of early modern humans from Layer 2 (Jin et al., 2009; Liu et al., 2010). This assemblage is central to both understanding later Pleistocene mammalian faunal transitions in southeastern Asia and, anthropocentrically, the timing of the appearance of early modern humans in eastern Asia.

Initially dated by U-series on flowstones directly above the fossiliferous layers, the *Homo* mandible and concomitant assemblage have been dated to be older than the early Late Pleistocene (MIS 5c). However, the maximum age of this assemblage is still unascertained. Here, we present our attempt to determine the maximum age of the fossils excavated from the Zhiren Cave by using paleomagnetic and optical simulated luminescence techniques to date the sediments which bracket the fossils, along with the previously obtained U-series dating results from the flowstones.

2. Geological and archaeological settings

The Zhiren Cave (*Homo sapiens* Cave) is located at an altitude of 179 m above sea level. It is developed in Triassic limestone, and consists of an open chamber and a tubular passage at the rear left of the cave. The sediments infilling Zhiren Cave consist of two stratified units (Fig. 1), which are separated by an easily recognizable erosive contact surface. The erosive contact surface was overlain by stalactites and flowstone (Jin et al., 2009). The upper unit is composed of intact sediments and is about 1.2 m in thickness. The lower one was deposited after the original filling sediments were partly eroded and is about 3.9 m thick. The lower unit is composed of six layers: a) The uppermost layer is composed of four distinct calcite layers; b) The second layer is solid yellowish brown sandy clay cemented by calcite with a few limestone breccias; c) The third layer is grayish brown silty clay with many iron-manganese nodules. A thin interrupted grayish-white calcite layer with various thicknesses (3–10 cm) lies between the second and third layers; d) The fourth layer is blocky yellowish-white silty clay with yellowish-brown iron mottling; e) The fifth layer is mainly grayish-white clay with few yellowish-brown iron mottling; f) The bottom layer consists of loosely cemented yellowish brown silt (Fig. 1). The *Homo* mandible and the associated *Elephas kiangnanensis*, *E.s maximus*, and *Megatapirus augustus*, and plentiful other mammalian fossils were excavated from the second layer, whereas abundant mammalian fossils were derived from the third layer (Jin et al., 2009).

3. Sampling and methodology

There are four layers of flowstone calcite overlying the sediments in which the human remains and faunal fossils were unearthed. These four layers of calcite deposits have been dated using ICP-MS U-series dating techniques to four time periods, around ~28, 52, 82 and 106 ka (Fig. 1). The age of the lowest speleothem calcite deposit provides the minimum age of 106 ka for the human remains and fauna assemblage (Liu et al., 2010). However, no suitable speleothem fragments were found for U-series dating within the lower layers *in situ*, leaving the maximum age as yet undetermined. To further anchor the maximum age of the human remains and the fossil fauna, 23 block samples were collected throughout Layers b) to f) in Zhiren Cave at stratigraphic intervals of 10–20 cm, and oriented by a magnetic compass in the field. Six samples for OSL dating were collected from Layers b) to f) in the lower unit. The depths of all these samples were measured from the cave ceiling (top of upper unit).

3.1. Palaeomagnetic analysis

All the oriented block samples for palaeomagnetic study were continuously sliced and oriented with intervals of 2 cm in depth and then cut into 3–6 cubic specimens of $2 \times 2 \times 2$ cm^3 in the laboratory. These discrete samples were then demagnetized using thermal demagnetization methods. As a rule, samples were stepwise heated to a maximum temperature of 680 °C with 10–50 °C temperature increments. The natural remnant magnetization (NRM) was measured after each thermal demagnetization step using a cryogenic superconducting magnetometer (model 2G-755R), which is installed in the magnetic shielded space (<150 nT), and the thermal demagnetization using a thermal demagnetizer (model ASC TD-48).

NRM intensities of the samples ranged from 4.5×10^{-6} to 1.7×10^{-5} A/m, well above the noise level of the magnetometer used, which is generally in the order of 10^{-8}–10^{-9} A/m. Demagnetization results were evaluated on stereographic projections and orthogonal diagrams, and the latter was used to resolve component structures (Zijderveld, 1967).

Principal component analysis (PCA) (Kirschvink, 1980), calculated with a least squares linear fit, and using the origin as a data point, was performed on the demagnetization data. The characteristic remnant magnetization (ChRM) directions were determined from at least four continuous steps (between 250 and 585 °C) with a maximum angular deviation (MAD) less than 15°. The principal component analyses (PCA) were conducted using the PaleoMag software developed by Jones (2002). Several representative samples were selected for further rock magnetic measurements. Using a MFK1-FA Kappabridge equipped with a CS-3 high-temperature furnace, temperature-dependent susceptibility (κ–T) curves were measured in an argon atmosphere from room temperature up to 700 °C and then back to room temperature. All experiments were finished at the Environmental Magnetism Laboratory of the Institute of Earth Environment, Chinese Academy of Sciences (IEECAS).

3.2. Optically stimulated luminescence (OSL) dating

Six samples were taken from Zhiren Cave for Optically Stimulated Luminescence (OSL) dating. In the laboratory, the samples were extracted under subdued red lighting, and pretreated with 30% HCl and 30% H_2O_2 to remove carbonates and organic material, respectively. The fine-grained (4–11 μm) quartz grains were then extracted from the bulk samples for luminescence dating (Lu et al., 2007). The purity of the quartz fraction was checked by infrared (IR) stimulation before construction of the growth curve and IR depletion method (Duller, 2003).

OSL measurements were conducted using a Daybreak 2200 reader equipped with a combined blue (470 ± 5 nm) and infrared (880 ± 80 nm) LED OSL unit, and $^{90}Sr/^{90}Y$ beta source (dose rate 0.090 Gy/s) for irradiation. All luminescence measurements were made at 125 °C for 50 s with both IR and blue stimulation powers at ~45 mW/cm^2. Luminescence emissions were detected by an EMI 9235QA photomultiplier tube and two 3 mm U-340 glass filters.

Equivalent dose (ED) was determined using sensitivity-corrected Multiple Aliquot Regenerative-dose protocol (Lu

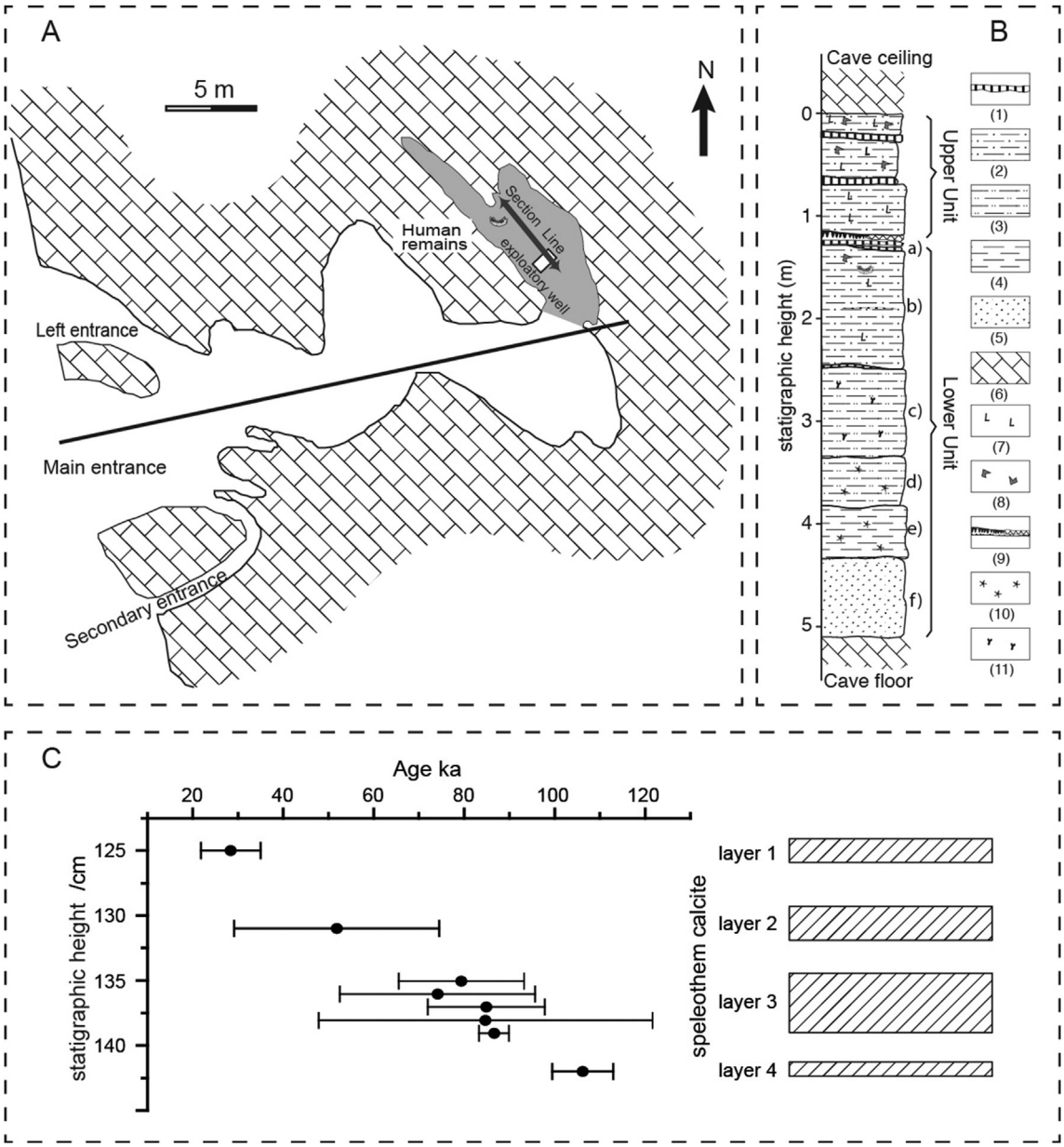

Fig. 1. A. Plan view of Zhirendong (Zhiren Cave). The gray area indicates the excavated area. Modified from Jin et al. (2009). B. Stratigraphy of the Zhiren cave section (reploted from the Jin et al., 2009). (1), Flowstone stone layers; (2) Sandy clay; (3) Silty clay; (4) Clay; (5) Siltite; (6) Limestone; (7) Calcite crystal; (8) Limestone braccia; (9) Erosive contact surface; (10) Iron mottling; (11) Iron-manganese nodules. C. Sketch showing the speleothem calcite layers overlying the sediments [the uppermost layer a) in panel B] and their U-series ages obtained previously (Liu et al., 2010).

et al., 2007), and more than 15 natural aliquots were used to measure natural OSL intensities and generally 6 regeneration doses were used to construct growth curve for each samples. For ED calculation, the first 5 s integral of the OSL decay curve was used after subtracting that of the last 5 s. Preheating temperatures for both natural or regeneration and test dose were 260 and 220 °C for 10 s, respectively. Fig. 2 shows the estimation of equivalent dose by a comparison of natural and regenerated OSL intensities using growth curve for all six samples. It can be seen that ED determination of 292 ± 4 Gy (sample IEE2734) is reliable, as the D0 of growth curve is 237 ± 19 Gy that enable OSL dating back to about 474 Gy, and for all six sample the average D0 is 226 ± 14 Gy.

The concentrations of uranium and thorium were measured using ICP-MS, whereas the potassium concentration was analyzed using ICP-OES at ChangAn University. Analytical precision was better than 3% for the uranium and thorium concentrations and better than 1% for the potassium concentration. The water contents, which varied from 6% to 18%, were calculated from the weight difference before and after drying of the fresh samples. The dose rate was calculated using the Dose4Win program supported by Prof. Andrzej Bluszcz (GADAM Centre of Excellence, Department of Radioisotopes, Institute of Physics, Silesian University of Technology) with alpha efficiency of 0.04 ± 0.01 and mean water content of 12 ± 5% of six samples. The original data and estimated OSL ages are given in Table 1.

Table 1
Summary of dosimetry and OSL ages of Lower Unit.

Lab no.	Depth (cm)	U (ppm)	Th (ppm)	K(%)	Water content (%)	Dose rate (Gy/ka)	ED (Gy)	Age (ka)
IEE2730	180	2.68	17.25	0.42	7.04	2.91 ± 0.16	343.8 ± 5.5	118.3 ± 6.6
IEE2731	240	4.64	27.70	0.89	13.17	4.66 ± 0.24	327.3 ± 16.8	70.2 ± 5.0
IEE2732	290	3.90	24.78	0.69	18.71	3.76 ± 0.19	314.8 ± 6.4	83.7 ± 4.6
IEE2733	400	4.86	28.00	0.87	12.82	4.74 ± 0.24	333.7 ± 1.1	70.3 ± 3.6
IEE2734	450	1.88	11.44	2.21	12.30	3.64 ± 0.15	291.7 ± 4.1	80.1 ± 3.4
IEE2735	480	1.08	6.78	1.86	7.76	2.80 ± 0.12	253.1 ± 2.8	90.3 ± 3.9

4. Results

4.1. Magnetic mineralogy and palaeomagnetism

A marked decrease of the magnetic susceptibility at about 580 °C and continuous declines from 580 °C to 700 °C are evident in the κ–T heating curves of all of the representative samples (Fig. 3), indicating the Curie temperature of magnetite and the occurrence of hematite respectively (Thompson and Oldfield, 1986; Dunlop and Ozdemir, 1997; Evans and Heller, 2003). The abrupt rise after 300–320 °C for the upper three samples at 2.02 m, 2.95 m and 3.67 m may be attributed to the thermal breakdown of greigite upon heating (Roberts et al., 2011), suggesting that these three samples have undergone some degree of post-depositional reductive diagenesis (Robinson et al., 2000). The steady descent heating curves below about 500 °C for the sample from 4.52 m may be ascribed to the presence of detrital, coarse-grained PSD/MD magnetic particles (Deng et al., 2000, 2005). The magnetic susceptibility

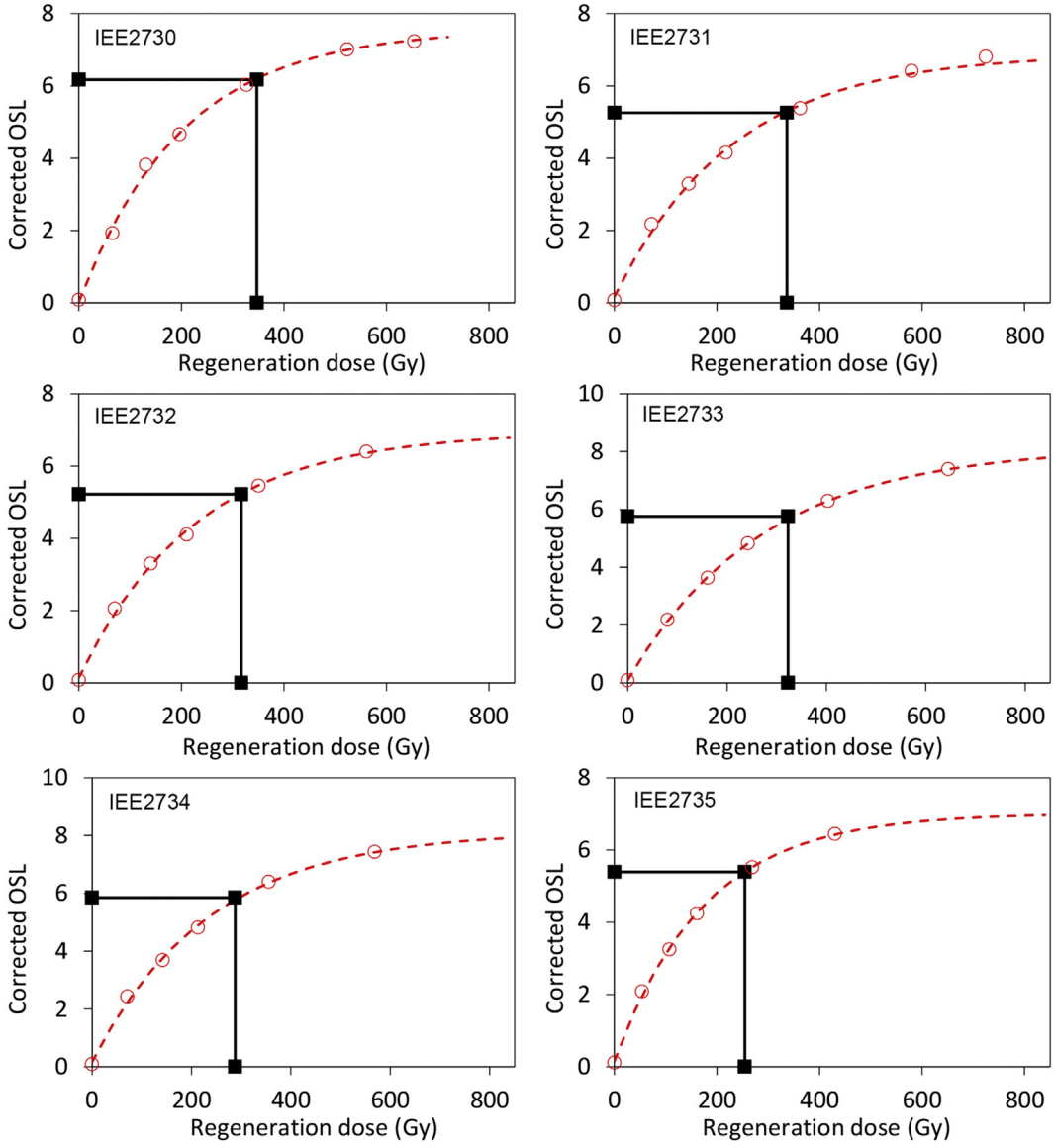

Fig. 2. ED determination for six OSL dating samples.

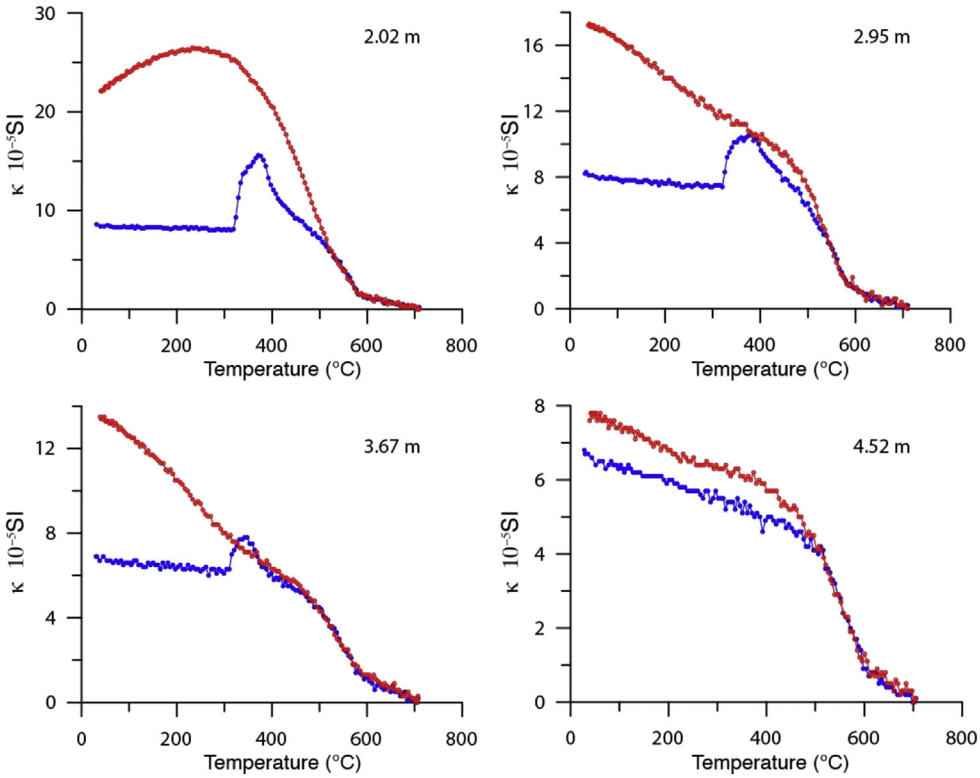

Fig. 3. Temperature dependence of initial susceptibility for samples from four representative intervals of the cave deposits. Red lines denote the heating curve, and blue lines indicate the cooling curve.

of all the heating and cooling curves is almost reversible at about 500–700 °C indicated that there is no conversion of the magnetic minerals. The magnetic susceptibility of the cooling curves increase below about 500 °C, apparently only caused by the thermal breakdown of greigite and conversion of coarse-grained PSD/MD magnetic particles of the samples.

In general, thermal demagnetizations can remove viscous components of magnetization around 250 °C, and hence obtain the characteristic remnant magnetization (ChRM). Fig. 4 shows orthogonal projections of remnant magnetization during progressive thermal demagnetization. The examples shown cover the full range of directional behavior exhibited during this study. Maximum angular deviation (MAD) values are generally less than 15°, indicating that the components are well defined (Fig. 5).

The detailed geomagnetic polarity sequence of the lower unit is established based on the thermal demagnetization. As shown in Fig. 5, all samples above 2.32 m have normal polarity. Below 2.32 m, most of samples have reversed polarities, while the declinations and inclinations of samples close to the bottom of the profile show some fluctuations. There are three samples, located at 4.4 m, which have positive declinations and fluctuating inclinations. The virtual geomagnetic pole (VGP) exhibited a deviation of more than 40° from the geographic pole, indicating a normal polarity period. Therefore, two excursional events can be identified with the calculated virtual geomagnetic pole (Fig. 5), although the beginning of the reversed polarity period at the bottom is hard to delineate.

4.2. OSL dating

Six OSL dates displayed a wide range of ages from ~70 to 126 ka (Table 1). Except for the uppermost sample (IEE2730), whose age (~126 ka) conforms with the U-series dates of the overlying flowstone, all of the ages are younger than the U-series dates and the uppermost OSL dates, even though these five OSL ages are generally consistent with the stratigraphic order. The upper 4 samples are clay and produced similar ED values, but their U and Th concentrations are different. The U and Th concentration of uppermost sample is about half of the following clay samples, resulting in the reduced dose rate estimation, which is based on the measured U, Th and K concentration, for the OSL age calculation.

The application of OSL dating inside this karst cave is suspected to be problematic, largely because of the uncertainty associated with the dose rate that was calculated from the concentrations of U, Th and K. The U-Th contents of the sediments could be altered by the addition of Uranium and Thorium through the drip water, and using the present U-Th contents may overestimate the dose rate of the samples. On the other hand, with the possible saturated water content and subsequent evaporation, the Radon daughter in decay chain would escape and induce the further overestimation of the dose rate. Therefore, using the present U-Th contents of the cave sediment could underestimate the age of the sediment inside the cave, due to the escape of Radon. For the sediments close to the surface of deposits, however, the reduced radiation caused by the escaped Radon may be compensated by the relatively higher Radon concentration in the cave air, which is the normal phenomena inside the karst cave (Cigna, 2005). Given these concerns, we do not consider these apparent ages obtained from the OSL dating to be reliable, due to the uncertainty associated with the estimation on the dose rate. However, it is noteworthy that corrected natural OSL intensities from six samples had never reached to the saturation level that was constructed by the laboratory dosing process. The ED values of these 6 samples should not be larger than ~600 Gy and the real geological ages of these 6 samples might be younger than ~210 ka (using the smallest dose rate of 2.8 Gy/ka), implying that 210 ka could be the lower boundary (maximum age) of the sediments.

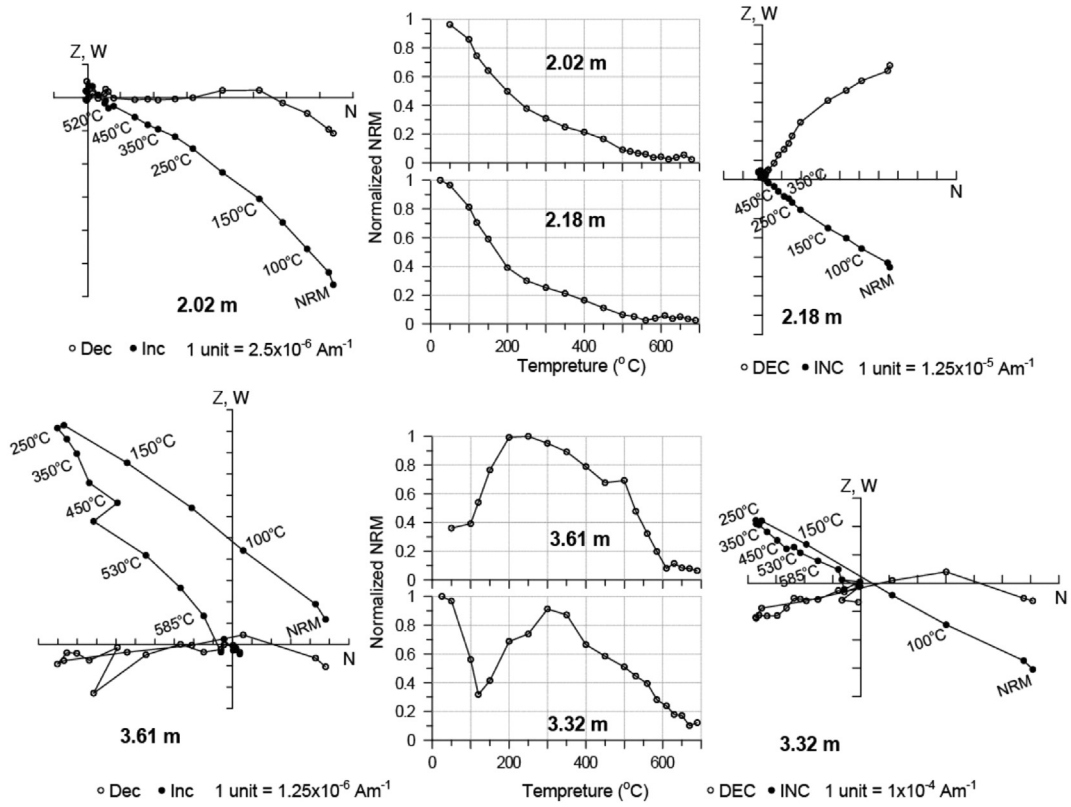

Fig. 4. Orthogonal projections of demagnetization data for representative samples from four intervals of the cave deposits. Open (closed) symbols represent vector end points projected on the vertical (horizontal) plane, respectively.

5. Discussion and conclusion

Paleomagnetic analyses reveal two reversed polarity zones below the fossiliferous layer, although the beginning of this event is not preserved, suggesting a rapid depositional process that is propitious to the burial and preservation of the fossils and an age close to that of the speleothem calcite. Thus, the age of these reversed polarity zones could be used as the maximum buried age of the fossils. Over the last 800 ka, the earth's magnetic polarity has been the Brunhes normal polarity chron. A series of reversed polarity excursions have been reported, and five excursions are well documented and have good age controls (Channell, 2006) during the last 300 ka. They are Mono Lake, Laschamp, Blake, Iceland Basin, and Pringle Falls and have ages of 32 ka, 41 ka, 120 ka, 185 ka, and 220 ka, respectively. The U-series dating of the flowstone calcite of layer overlying the fossil-contained layers provides a minimum age for the lower unit in Zhiren Cave, ~106 ka. The OSL measurements suggest that the maximum age of the lower unit should be younger than 210 ka. It is therefore evident that the reversed polarity excursions observed in this profile is older than 106 ka and likely younger than 210 ka, and it could be correlated to any one of the three events: the Blake, Iceland Basin, and probably Pringle Falls excursions fall within this period. Fig. 6 shows the VGP path of the reverse excursions observed at Zhiren Cave. It consists of a southward swing through North and South America, followed by a loop through the Indian Ocean and central Asia. The path morphology is similar to that of the previously reported Blake event, but not that of the Iceland Basin and Pringle Falls (Valet et al., 2008, references therein). We therefore argue that the reverse event found in Zhiren Cave most likely corresponds to the Blake excursion. In addition, the Blake excursion has also been recorded as two reverse polarity zones in Mediterranean and Chinese loess (Tric et al., 1991; Fang et al., 1997) and by stalagmites in northern Spain, which provide accurate U-series ages of 112.0–116.5 ka for the Blake event (Osete et al., 2012). Two reverse polarity zones found in this profile also lend some supports to the identification of the Blake excursion in Zhiren Cave. Therefore, the human remains and the mammalian fauna assemblage can be bracketed to 116–106 ka.

The Zhiren fauna lacks *Gigantopithecus blacki*, *Sinomastodon*, *Ailuropoda*, and *Stegodon*, and it has advanced forms such as *Elephas maximus* and *Bandicota indica*. Its features are distinctly different from the Early Pleistocene *Gigantopithecus* fauna and the Middle Pleistocene *Ailuropoda-Stegodon* fauna(s.s.). The fauna is a transitional one between the typical *Ailuropoda-Stegodon* fauna (s.s.) and the Asian elephant fauna, and also could be regarded as an early representative of the typical Asian elephant fauna (Jin et al., 2009; Zhao et al., 2009; Wang et al., 2010). The fauna excavated from Zhiren Cave is characterized by a lack of forest animal species, while it is dominated by a multitude muroid rodents (such as *Bandicota* and *Rattus*), probably indicating at that time that the forest was reduced while the grassland expanded, i.e., a relatively cool and dry condition. Considering the Asian summer monsoon was weakened during MIS 5d (~120–110 ka, Cai et al., 2015, references therein), it is very likely that this fauna inhabited this region in MIS 5d, further supporting our estimation of the ages of the fossils. In summary, the human and fauna were very likely deposited during MIS 5d (~116–110 ka), making it the oldest human fossil with distinctly modern features in eastern Asia. The ages bracketing the Zhiren Cave remains provide a chronological framework for assessing the population processes associated with the establishment of modern human biology in the region.

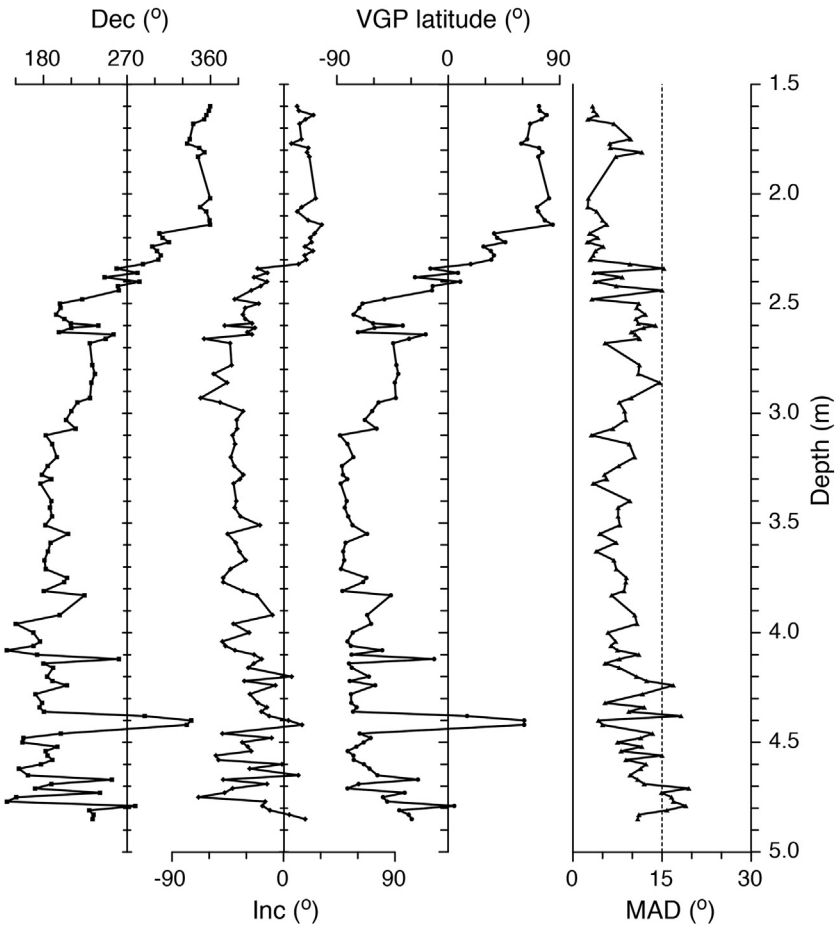

Fig. 5. Component declination, inclination, VGP latitude and accompanying maximum angular deviation (MAD) values of the cave deposits below the flowstone.

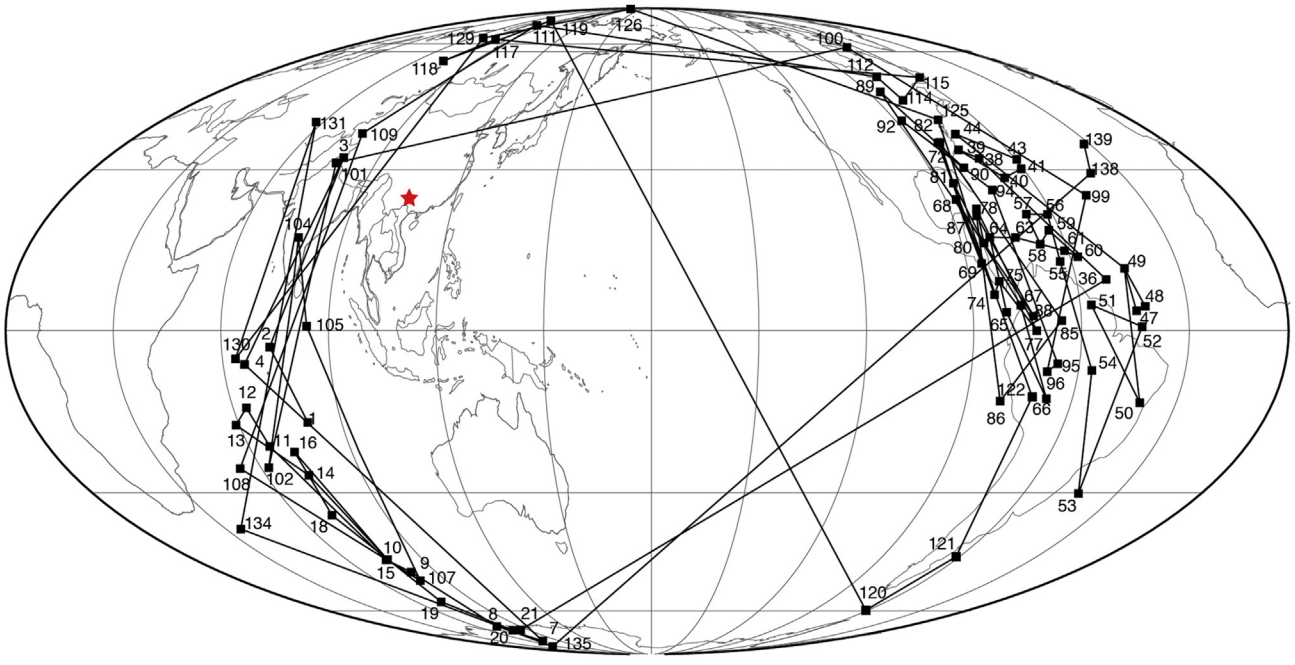

Fig. 6. VGP path of the reversal excursions observed in the Zhiren Cave. A southward swing through North and South America is followed by a loop through the Indian Ocean and central Asia. Star indicates Zhiren Cave.

Acknowledgements

We thank Profs. Pan W S and Qin D G from Peking University for field sampling assistance. This work was supported by National Natural Science Foundation of China grants (41271229, 41572164) and the grants from Chinese Academy of Sciences (KZZD-EW-04-01).

References

Cai, Y., Fung, I.Y., Edwards, R.L., An, Z., Cheng, H., Lee, J.-E., Tan, L., Shen, C.-C., Wang, X., Day, J.A., 2015. Variability of stalagmite-inferred Indian monsoon precipitation over the past 252,000 y. Proceedings of the National Academy of Sciences 112, 2954–2959.

Channell, J.E.T., 2006. Late Brunhes polarity excursions (Mono Lake, Laschamp, Iceland Basin and Pringle falls) recorded at ODP site 919 (Irminger Basin). Earth and Planetary Science Letters 244, 378–393.

Cigna, A.,A., 2005. Radon in caves. International Journal of Speleology 34 (1–2), 1–18.

Deng, C., Vidic, N.J., Verosub, K.L., Singer, M.J., Liu, Q., Shaw, J., Zhu, R., 2005. Mineral magnetic variation of the Jiaodao Chinese loess/paleosol sequence and its bearing on long-term climatic variability. Journal of Geophysical Research, Solid Earth 110, B03103.

Deng, C., Zhu, R., Verosub, K.L., Singer, M.J., Yuan, B., 2000. Paleoclimatic significance of the temperature-dependent susceptibility of Holocene loess along a NW-SE transect in the Chinese loess plateau. Geophysical Research Letters 27, 3715–3718.

Duller, G.A.T., 2003. Distinguishing quartz and feldspar in single grain luminescence measurements. Radiation Measurements 37, 161–165.

Dunlop, D.J., Özdemir, Ö., 1997. Rock Magnetism: Fundamentals and Frontiers. Cambridge Univ. Press, Cambridge, U. K.. http://dx.doi.org/10.1017/CBO9780511612794

Evans, M.E., Heller, F., 2003. Environmental Magnetism: Principles and Applications of Enviromagnetics. Academic, San Diego, California.

Fang, X., Li, J., Van der Voo, R., MacNiocaill, C., Dai, X., Kemp, R.A., Derbyshire, E., Cao, J., Wang, J., Wang, G., 1997. A record of the Blake Event during the last interglacial paleosol in the western loess plateau of China. Earth and Planetary Science Letters 146, 73–82.

Fu, Q., Meyer, M., Gao, X., Stenzel, U., Burbano, H.A., Kelso, J., Pääbo, S., 2013. DNA analysis of an early modern human from Tianyuan Cave, China. Proceedings of the National Academy of Sciences USA 110, 2223–2227.

Fu, Q., Li, H., Moorjani, P., Jay, F., Slepchenko, S.M., Bondarev, A.A., Johnson, P.L.F., Aximu-Petri, A., Prüfer, K., de Filippo, C., Meyer, M., Zwyns, N., Salazar-García, D.C., Kuzmin, Y.V., Keates, S.G., Kosintsev, P.A., Razhev, D.I., Richards, M.P., Peristov, N.V., Lachmann, M., Douka, K., Higham, T.F.G., Slatkin, M., Hublin, J.J., Reich, D., Kelso, J., Viola, T.B., Pääbo, S., 2014. Genome sequence of a 45,000-year-old modern human from western Siberia. Nature 514, 445–450.

Fu, Q., Hajdinjak, M., Moldovan, O.T., Constantin, S., Mallick, S., Skoglund, P., Patterson, N., Rohland, N., Lazaridis, I., Nickel, B., Viola, B., Prüfer, K., Meyer, M., Kelso, J., Reich, D., Pääbo, S., 2015. An early modern human from Romania with a recent Neanderthal ancestor. Nature 524, 216–220.

Jin, C.Z., Pan, W.S., Zhang, Y.Q., Cai, Y.J., Xu, Q.Q., Tang, Z.L., Wang, W., Wang, Y., Liu, J.Y., Qin, D.G., Edwards, R.L., Cheng, H., 2009. The Homo sapiens cave hominin site of Mulan Mountain, Jiangzhou District, Chongzuo, Guangxi with emphasis on its age. Chinese Science Bulletin 54, 3848–3856.

Jones, C.H., 2002. User-driven integrated software lives: "PaleoMag" Paleomagnetics analysis on the Macintosh. Computers and Geosciences 28 (10), 1145–1151.

Kirschvink, J.L., 1980. The least squares lines and plane analysis of paleomagnetic data. Geophysical Journal Royal Astronomical Society 62, 699–718.

Liu, W., Jin, C.-Z., Zhang, Y.-Q., Cai, Y.-J., Xing, S., Wu, X.-J., Cheng, H., Edwards, R.L., Pan, W.-S., Qin, D.-G., An, Z.-S., Trinkaus, E., Wu, X.-Z., 2010. Human remains from Zhirendong, South China, and modern human emergence in East Asia. Proceedings of the National Academy of Sciences 107, 19201–19206.

Lu, Y.C., Wang, X.L., Wintle, A.G., 2007. A new OSL chronology for dust accumulation in the last 130,000 yr for the Chinese Loess Plateau. Quaternary Research 67, 152–160.

Osete, M.-L., Martín-Chivelet, J., Rossi, C., Edwards, R.L., Egli, R., Muñoz-García, M.B., Wang, X., Pavón-Carrasco, F.J., Heller, F., 2012. The Blake geomagnetic excursion recorded in a radiometrically dated speleothem. Earth and Planetary Science Letters 353–354, 173–181.

Roberts, A.P., Chang, L., Rowan, C.J., Horng, C.-S., Florindo, F., 2011. Magnetic properties of sedimentary greigite (Fe_3S_4): an update. Reviews of Geophysics 49 (1), 1–46.

Robinson, S.G., Sahota, J.T.S., Oldfield, F., 2000. Early diagenesis in North Atlantic abyssal plain sediments characterized by rock-magnetic and geochemical indices. Marine Geology 163, 77–107.

Shang, H., Trinkaus, E., 2010. The Early Modern Human from Tianyuan Cave, China. Texas A&M University Press, College Station.

Smith, F.H., Janković, I., Karavanić, I., 2005. The assimilation model, modern human origins in Europe, and the extinction of Neandertals. Quaternary International 137, 7–19.

Thompson, R., Oldfield, F., 1986. Environmental Magnetism. Allen and Unwin, Winchester, Mass. http://dx.doi.org/10.1007/978-94-011-8036-8.

Tric, E., Laj, C., Valet, J.-P., Tucholka, P., Paterne, M., Gichard, F., 1991. The Blake geomagnetic event: transition geometry, dynamical characteristics and geomagnetic significance. Earth and Planetary Science Letters 102, 1–13.

Trinkaus, E., 2005. Early modern humans. Annual Review of Anthropology 34, 207–230.

Trinkaus, E., 2007. European early modern humans and the fate of the Neandertals. Proceedings of the National Academy of Sciences 104, 7367–7372.

Valet, J.P., Plenier, G., Herrero-Bervera, E., 2008. Geomagnetic excursions reflect an aborted polarity state. Earth & Planetary Science Letters 274, 472–478.

Wang, Y., Jin, C.Z., Zhang, Y.Q., Qin, D.G., 2010. Murid rodents from the *Homo sapiens* cave of Mulan Mountain, Chongzuo, Guangxi, South China. Acta Anthropologica Sinica 29 (3), 303–316 (in Chinese with English abstract).

Wu, X., 2004. On the origin of modern humans in China. Quaternary International 117, 131–140.

Zhao, L.X., Wang, C.B., Jin, C.Z., Qin, D.G., Pan, W.S., 2009. Fossil Orangutan-like hominoid teeth from Late Pleistocene human site of Mulanshan cave in Chongzuo of Guangxi and implications on taxonomy and evolution of orangutan. Chinese Science Bulletin 54, 3924–3930.

Zijderveld, J.D.A., 1967. AC demagnetization of rocks: analysis of results. In: Collinson, D.W., Creer, K.M., Runcorn, S.K. (Eds.), Methods on Paleomagnetic. Elsevier, Amsterdam, pp. 254–286.